

HARD X-RAY AND METRIC/DECIMETRIC SPATIALLY RESOLVED OBSERVATIONS OF THE 10 APRIL 2002 SOLAR FLARE

N. Vilmer¹, S. Krucker², G. Trottet¹ and R.P. Lin²

¹*LESIA, Observatoire de Paris, 92195- Meudon- Cedex, France*

²*Space Sciences Laboratory, University of California, Berkeley, CA-94720, USA*

ABSTRACT

The GOES M8.2 flare on 10 April 2002 at ~ 1230 UT was observed at X-ray wavelengths by RHESSI and at metric/decimetric wavelengths by the Nançay Radioheliograph (NRH). We discuss the temporal evolution of X-ray sources together with the evolution of the radio emission sites observed at different coronal heights by the NRH. While the first strong HXR peak at energies above 50 keV arises from energy release in compact magnetic structures (with spatial scales of a few 10^4 km) and is not associated with strong radio emission, the second one leads to energy release in magnetic structures with scales larger than 10^5 km and is associated with intense decimetric/metric and dekametric emissions. We discuss these observations in the context of the acceleration sites of energetic electrons interacting at the Sun and of escaping ones.

INTRODUCTION

Complementary observations of solar flare hard X-ray (HXR) emitting electrons are provided by the radio emission of non thermal electrons produced in a wide range of coronal heights and in a wide frequency range from a few tens of GHz to a few MHz (see e.g. Bastian et al., 1998; Vilmer and MacKinnon, 2003, Trottet, this volume for reviews). While HXR and centimetre/millimetre wave emissions are the most direct diagnostics of the energetic electrons in the chromosphere and low corona, the coherent plasma radiations such as the ones emitted at greater coronal heights (10^4 - 10^5 km) in the metric/decimetric domain are a sensitive diagnostic of electrons of a few tens of keV injected in the corona from the flare site. These radio observations combined with X-ray/EUV measurements contain unique information on the various circumstances of electron acceleration in the solar atmosphere and on the coronal sites of electron acceleration (see e.g. Klein et al., 2001).

INSTRUMENTATION

The HXR and metric/decimetric imaging observations of the 10 April 2002 solar flare were obtained respectively by the RHESSI instrument (Lin et al., 2002) and by the Nançay Radioheliograph (NRH) at 432, 410, 327, 236 and 164 MHz (Kerdraon and Delouis, 1996). Radio spectra from ~ 4 GHz to ~ 1 MHz were obtained respectively by the Phoenix-2 spectrometer operated by ETH Zürich (Messmer et al., 1999), the radio spectrometer from AIP Potsdam (OSRA) (Mann et al., 1992) and by the WAVES experiment aboard the WIND spacecraft (Bougeret et al., 1995). The EUV image obtained shortly before the flare at 195Å by the Extreme Ultraviolet Telescope (EIT) aboard SOHO (Delaboudinière et al., 1995) is also used to provide complementary information on the context in which emission from non thermal electrons occurred.

OBSERVATIONS

Temporal Evolution of the Flare at X-Ray and Metric/Decimetric Wavelengths

The GOES M8.2 flare on 10 April 2002 at $\sim 12:30$ UT occurred in NOAA region 9901. Figure 1 shows the time evolution of the GOES X-ray flare, together with the RHESSI counts (not background subtracted) in the 50-100 keV energy band and the X-ray spectrogram (background subtracted) from ~ 3 keV to ~ 200 keV. For these observations, thin shutters were placed in front of the RHESSI detectors leading to a decrease in the efficiency for measuring photons below ~ 10 keV. The three bottom plots represent a composite radio spectrum from PHOENIX-2 in the 4 GHz-100 MHz range, OSRA (Potsdam) from 400 MHz to 40 MHz and the radio spectrum from WIND/WAVES in the 1-14 MHz band. Figure 2 shows the time evolution of the X-ray count rates in 4 energy bands together with the metric/decimetric radio flux observed at five frequencies with the Nançay Radioheliograph. For most of the event (from $\sim 12:28$ UT to $\sim 12:36$ UT) the high count-rate at low energies introduces pulse pile up effects in the ~ 25 to ~ 50 keV energy range. These effects have been corrected to first order in Figure 2. At energies above 50 keV, X-ray emission presents two main peaks: one observed around 12:28 UT which extends above 100 keV and a second less energetic one observed shortly after 12:30 UT. A fainter peak is observed at $\sim 12:27$ UT.

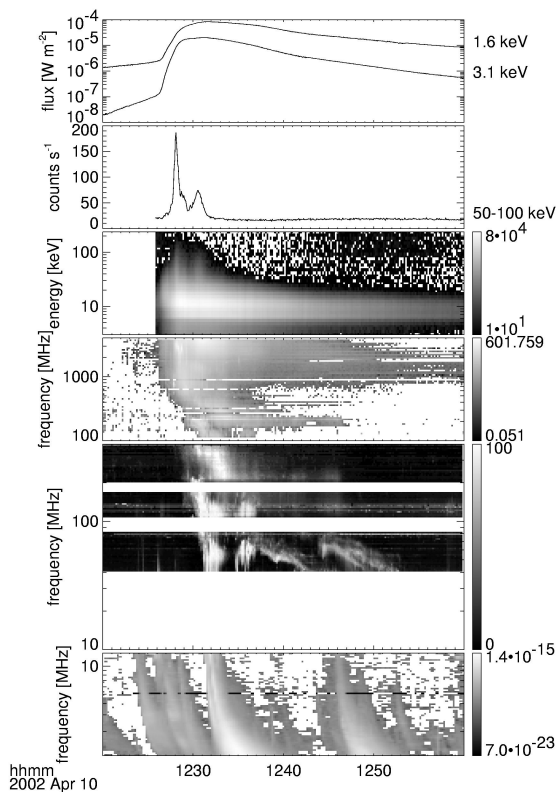


Fig1: from top to bottom:

- Time evolution of the GOES X-ray flux (panel 1) and of the X-ray RHESSI counts accumulated over 4s in the 50-100 keV energy band (background not subtracted) (panel 2)
- RHESSI X-ray spectrogram showing the evolution with time and photon energy of the X-ray emission (background subtracted) (panel 3)
- Radio composite spectrum observed between 4 GHz to 1 MHz by PHOENIX-2 (ETH Zürich) (panel 4), OSRA (AIP Potsdam) (panel 5) and the WIND/WAVES experiment (panel 6) (the time is in UT).

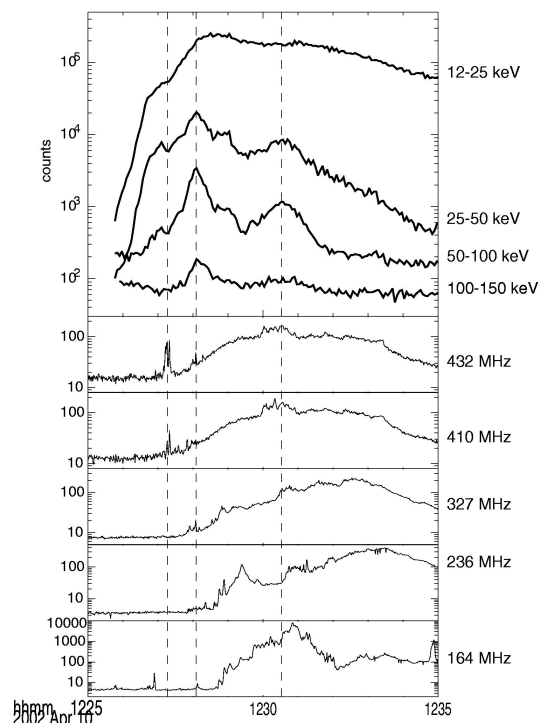


Fig 2: from top to bottom

- Time evolution of the X-ray RHESSI count-rates in 4 energy bands. The background is not subtracted but pile up effects have been corrected to first order. The accumulation time is 4s.
- Decimetric/metric radio flux observed in the flare region by the Nançay Radioheliograph (NRH) with an integration time of 1s (the time is in UT). The dashed vertical lines indicate the first radio 432 MHz burst at 12:27:20 UT and the two main HXR peaks above 50 keV around 12:28 UT and after 12:30 UT.

Above 1000 MHz, PHOENIX observations show a strong radio emission (most probably gyrosynchrotron radiation) closely associated in time with the most energetic X-ray emission. In the frequency range around 400 MHz, the emission starts at $\sim 12:27:20$ UT with a weak burst and then gradually rises from 12:28 UT (Figure 2). At lower frequencies (below 300 MHz), faint radio emission starts after 12:28 UT (i.e. after the most energetic X-ray peak), the onset time of the lowest frequencies being progressively delayed (Figures 1 and 2). A strong increase of the radio emission is observed around $\sim 12:31$ UT and consists of type III bursts followed several minutes later by type II bursts. The type III bursts around 12:31 UT extend below 14 MHz showing electron beams injection towards the corona at heights much larger than $1 R_s$ above the photosphere. As seen in Figure 2, the strong radio emission observed at 164 MHz around 12:31 UT corresponds to flux enhancements above the gradually rising component seen shortly after 12:30 UT (close to the second main X-ray peak above 50 keV) at frequencies around 400 MHz. In summary, the second HXR peak is associated with stronger radio emission at frequencies below 300 MHz than the first one.

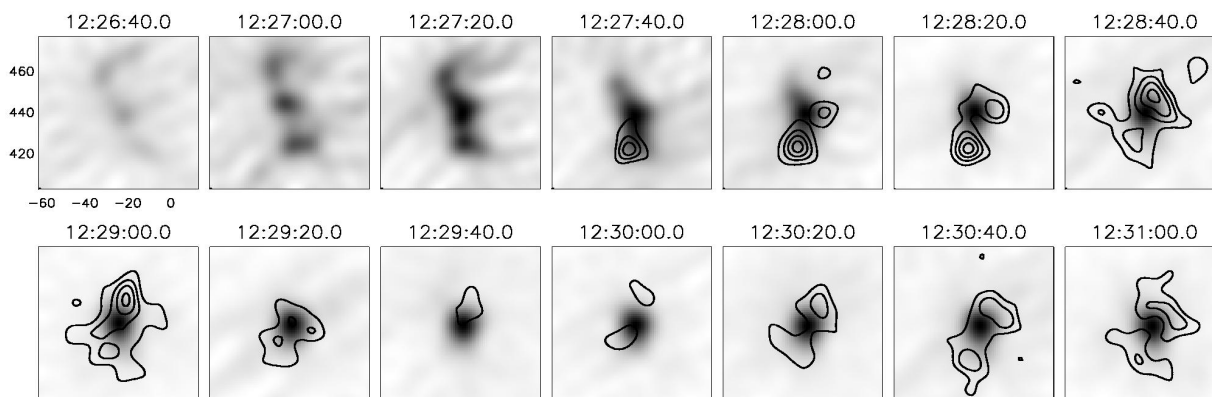


Fig 3: Time series of RHESSI images at 12-25 keV with HXR contours at 40-65 keV overlaid (30, 50, 70, 90 % of the maximum in each image). The field is $75'' \times 75''$. RHESSI images and contours are obtained using grids 3 to 9 giving a resolution of $7''$.

HXR and Decimetric/Metric Imaging Observations

Figure 3 shows X-ray images at 12-25 keV combined with contours at 40-65 keV obtained after 12:27:40 UT (i.e. with sufficient counts statistics in this energy range). The X-ray emission at 40-65 keV comes primarily from two sources with different temporal evolutions. It cannot be excluded however that these sources may be unresolved at the resolution of $7''$ shown here (see e.g. the observations of the 20 February 2002 by Krucker and Lin, 2002). The southernmost X-ray source at 40-65 keV is found to brighten earlier in the flare. Later on a northern component appears, becomes more extended in size (around 25000 km) and predominant at $\sim 12:28:40$ UT and around 12:30:20 UT.

Figure 4 shows combined contours of X-ray and decimetric radio emissions at 432 MHz. The contours are superposed on the same EIT image taken shortly before the HXR flare to provide information on the context in which emission from non thermal electrons arises. The RHESSI contours (indicated by X and black arrows) are shown for the 12-25 keV range early in the flare and for the 40-65 keV range after 12:28 UT. The southernmost X-ray component overlays bright EIT structures and is co-spatial with the EIT flare location observed in the next EIT frame at 12:36 UT. The northernmost component is located further away (around 20000 km) from these bright and compact EIT features. This northern component appears around 12:28:00 UT at 40-65 keV (image 4 in figure 3), i.e. at the peak time of the first main HXR peak above 50 keV. After 12:28:02 UT, this northern X-ray source is located at the base of an EIT loop (half length of the order of $7 \cdot 10^4$ km) and is dominant at $\sim 12:30:20$ UT, i.e. during the second HXR peak (see Figure 3 and image 6 of Figure 4). This north component at 40-65 keV is also not co-spatial with the X-ray emission at 12-25 keV during the fainter peak observed at 12:27 UT.

Figures 1 and 2 show that around 400 MHz the emission starts with narrowband bursts observed around 12:27:10 UT, i.e. about one minute later than the X-ray emission in the 12-50 keV range (image 3 of Figure 4). As already noted, the predominant X-ray peak at $\sim 12:28$ UT is not associated with a strong radio counterpart. Very faint bursts are however seen in the flux time profile (image 4 of Figure 4) corresponding to a new radio source.

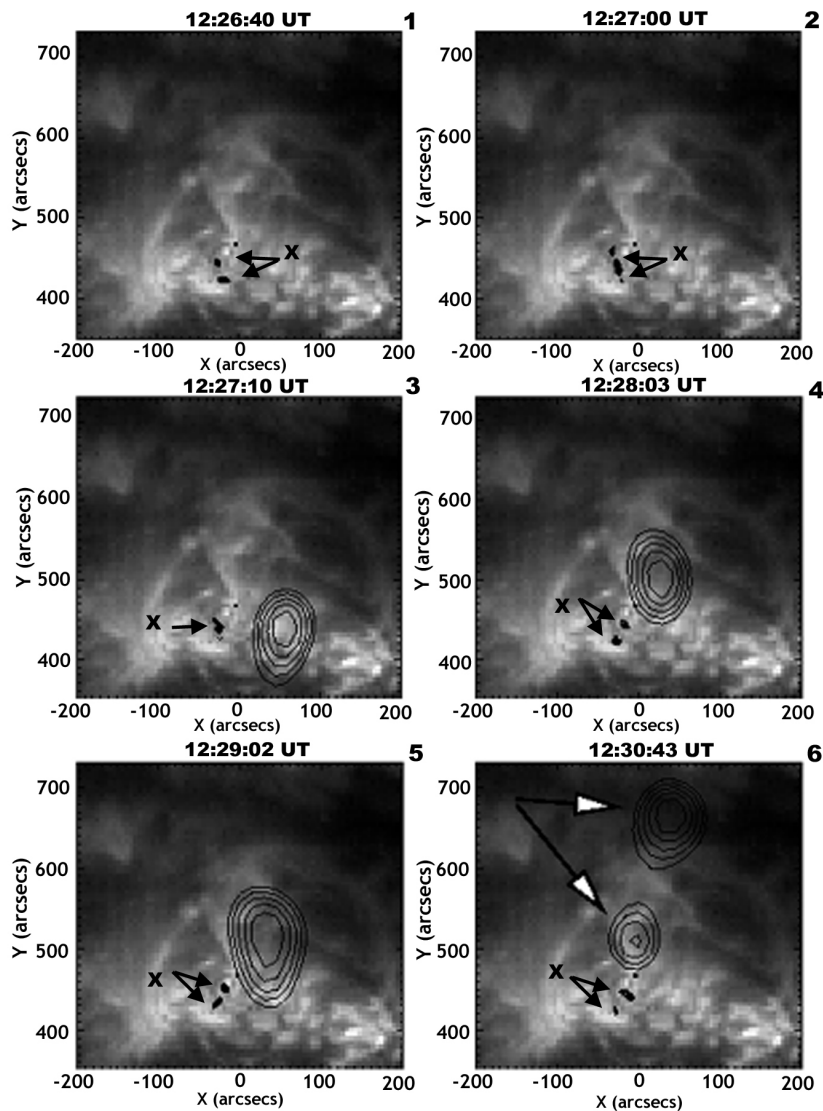


Fig 4: RHESSI iso-contours (thick black) (75,80,85,90,95 % of the maximum) and NRH contours at 432 MHz (thin black) overlaid on the EIT image at 12:24 UT (shortly before the flare). The RHESSI contours (x) are obtained using grids 3 to 9 giving a resolution of 7'' and are indicated by black arrows. They are shown for the 12-25 keV energy range for the first three images and for the 40-65 keV range for the last three images. Note the two components (white arrows) of the 432 MHz radio emission in the last image.

The location of the 432 MHz radio source changes between images 3 and 4 together with the appearance of the northern X-ray component at 40-65 keV. Such coincident changes in the morphology of HXR and decimetric sources have been reported previously for another flare (Vilmer et al., 2002). From 12:28 to 12:30 UT (images 4 and 5 of Figure 4), the 432 MHz radio source remains at this same position overlying the EIT loop with the northern HXR component at its base. The next major change in the configuration of the radio sources occurs around 12:30:43 UT, i.e. at the time of the second major HXR peak and of the enhancement of the 432 MHz flux (image 6 of Figure 4). A second radio component appears further from the active region much more to the north. From this time and until 12:33 UT, these two radio components are observed with varying relative intensities. After that time, the radio emission is predominantly coming from the southernmost component.

Around ~ 300 MHz the emission starts late in the flare development. The large X-ray peak at 12:28 UT is associated with a faint radio source (images 1 and 2 of Figure 5). At 164 MHz, faint radio emission is observed still at later times (from 12:28:40 UT). The position of the 164 MHz source changes at 12:29:43 UT, i.e.

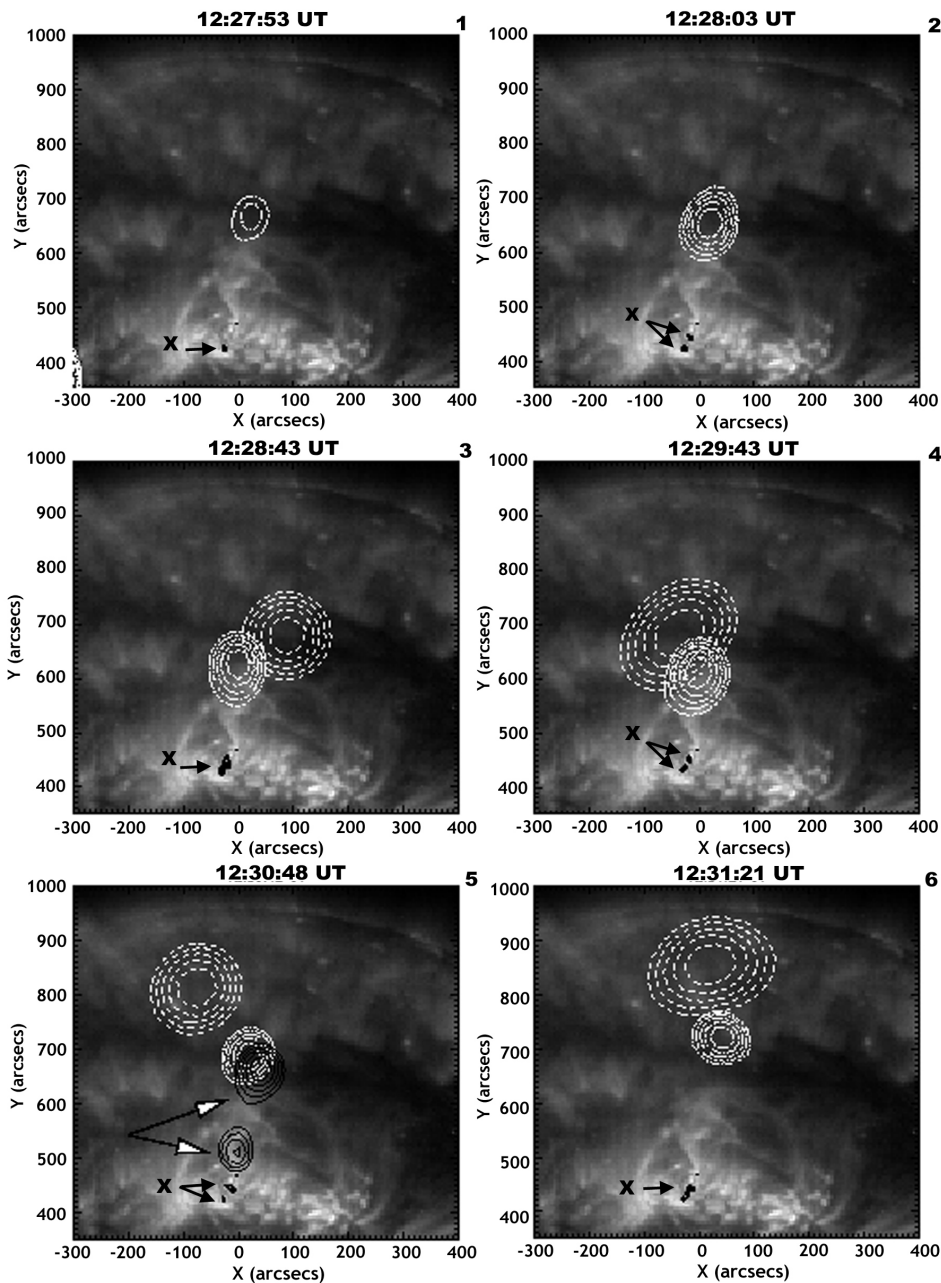


Fig 5: RHESSI iso-contours (thick black) (75,80,85,90,95 % of the maximum) and NRH contours at 327 MHz (dashed-dotted white) (75,80,85,90,95 % of the maximum) and 164 MHz (dotted white) (75,80,85,90,95 % of the maximum) observed at different times. Note that the 164 MHz emission appears later in the flare (from image 3). The two components at 432 MHz (indicated by arrows) are overlaid for comparison (black contours) in image 5. The RHESSI and NRH contours are overlaid on the EIT image obtained shortly before the flare at 12:24 UT. The RHESSI contours (x) are obtained in the 40-65 keV range using grids 3 to 9 (7'' resolution) and are indicated by black arrows.

together with the significant increase of the 164 MHz flux (see figure 2). A stronger increase of radio emission around and below 100 MHz finally occurs after 12:30 UT at the time of the second HXR peak together with another change in the radio emission pattern: the second component appears at 432 MHz and the radio sources at 327 and 164 MHz jump to the north (images 5 and 6 of Figure 5). These northern radio components are seen at the time of the strong radio emission extending below 14 MHz and may trace the electron path to the high ($> 1 R_s$ above the photosphere) corona and towards interplanetary space. After 12:32 UT, the radio sources at 164 MHz and 327 MHz remain located to the north and at 164 MHz the radio emission pattern becomes quite complicated exhibiting larger scale fainter features not discussed here.

Summary of the Observations and Discussion

This paper presents new spatially resolved observations of HXR and decimetric/metric emissions for the GOES M8.2 10 April 2002 solar flare. The observational results are summarized below:

- Although decimetric (432 MHz) emission starts shortly after the first peak above 50 keV at ~12:27 UT, radio emission at lower frequencies (i.e. below 300 MHz) start progressively later and after the most energetic HXR peak observed above 100 keV. This HXR peak is associated with very weak radio emission. This is consistent with the fact that 10 to 15 % of HXR producing electrons have no detectable emission at decimeter and longer wavelengths (e.g. Simnett and Benz, 1986). For this part of the event (i.e. before 12:30 UT), energetic electrons are confined in low lying loops (heights of several 10^4 km) with no access to the higher ($>10^5$ km) corona. This is consistent with the observations of the predominant southern compact ($\sim 10^4$ km) X-ray source during the most energetic HXR peak and of the decimetric sources overlying EIT loops with scales smaller than 10^5 km.

- Comparison of HXR images above 40 keV between the rising phase of the X-ray emission ($< 12:28$ UT) and the most energetic HXR peak shows the appearance of a new source above 40 keV which is not cospatial with previous X-ray sources at 12-25 keV. This behaviour is similar to what has been previously observed in some flares with SMM/HXIS (e.g. Machado et al., 1988) or YOHKOH/HXT (Raulin et al., 2000). A coincident change in the morphology of the decimetric source is also observed (images 3 and 4 of figure 4). This indicates a causal relationship between radio and HXR emitting sites attributed to variations in the energy release and electron injection sites (see also Vilmer et al., 2002).

- During the last HXR peak above 50 keV, the northern and more elongated X-ray component is slightly more intense than the southern one. This HXR peak is associated with the appearance of new radio components at all frequencies further away from the active region and corresponding to intense radio emission in the metric domain. This second peak thus results from energy release in different magnetic structures than the first ones and larger scales ($>10^5$ km) are now involved in the process. These new radio components further away from the active region appear at the time of the extension of strong radio emission below 14 MHz and may trace electron beam injection towards the even higher ($> 1 R_s$) corona and the interplanetary medium.

The two main HXR peaks observed above 50 keV in this event show two different episodes of energy release and electron acceleration. The first one occurring in compact (\sim a few 10^4 km) magnetic structures is responsible for the hardest part of the event in terms of electrons interacting at the Sun. The second one is less efficient for producing the most energetic electrons interacting at the Sun but leads to electron injection in both low lying (several 10^4 km) structures and in much larger scale features ($>10^5$ km) leading to radio emission at lower frequencies (down to 10 MHz). This second episode is a candidate for the injection of energetic electrons in the high corona ($> 1 R_s$) towards interplanetary space. Such an observation demonstrates the potentiality of combining RHESSI and NRH observations to understand the link between the production of energetic electrons interacting at the Sun and the injection of the escaping electrons giving rise to the radio emissions at the lowest frequencies.

REFERENCES

- Bastian, T., A.O. Benz, and D.E. Gary, Radio emission from solar flares, *Annual Review of Astron. Astrophys.*, **36**, 131-188, 1998.
- Bougeret, J.L., M.L. Kaiser, P.J. Kellogg, P.J. et al., Waves: the radio and plasma wave investigation on the Wind spacecraft, *Space Science Reviews*, **71**, 231-263, 1995.
- Delaboudinière, J.P., G.E. Artzner, J. Brunaud et al., EIT: Extreme-Ultraviolet Imaging Telescope for the SOHO mission, *Solar Phys.*, **162**, 291-312, 1995.
- Kerdran, A., and J.M. Delouis, The Nançay Radioheliograph, in *Coronal Physics from Radio and Space Observations*, edited by G. Trottet, pp. 192-201, Springer-Verlag, Heidelberg, Germany, 1997.
- Klein, K.L., G. Trottet, P.Lantos et al., Coronal electron acceleration and relativistic proton production during the 14 July 2000 flare and CME, *Astron. Astrophys.*, **373**, 1073-1082, 2001.
- Krucker, S., and R.P. Lin, Relative timing and spectra of solar flare hard X-ray sources, *Solar Phys.*, **210**, 229-243, 2002.
- Lin R.P., B.R. Dennis, G.J. Hurford et al., The Reuven Ramaty High-Energy Solar Spectroscopic Imager (RHESSI), *Solar Phys.*, **210**, 3-32, 2002

- Machado, M.E., R.L. Moore, A.M. Hernandez et al., The observed characteristics of flare energy release. I – Magnetic structure at the energy release site, *Astrophys. J.*, **326**, 425-450, 1988.
- Mann, G., H. Aurass, W. Voigt et al., Preliminary observations of solar type 2 bursts with the new radiospectrograph in Trossdorf (Germany), in *ESA, Proceedings of the First SOHO Workshop: Coronal Streamers, Coronal Loops, and Coronal and Solar Wind Composition*, pp 129-132, 1992.
- Messmer, P., A.O. Benz, and C. Monstein, PHOENIX-2: A New Broadband Spectrometer for Decimetric and Microwave Radio Bursts - First Results, *Solar Phys.*, **187**, 335-345, 1999.
- Raulin, J.P., N. Vilmer, G. Trottet et al., Small and large scale magnetic structures involved in the development of the 1992 October 28 solar flare, *Astron. Astrophys.*, **355**, 355-364, 2000.
- Simnett, G., M. and A.O. Benz, The role of metric and decimetric radio emission in the understanding of solar flares, *Astron. Astrophys.*, **165**, 227-234, 1986.
- Vilmer, N. and A.L. MacKinnon, A.L., What can be learned about competing acceleration models from multiwavelength observations?, in *Energy Conversion and Particle Acceleration in the Solar Corona*, edited by K.L. Klein, pp 127-160, Springer-Verlag, Heidelberg, Germany, 2003.
- Vilmer, N., S. Krucker, R.P. Lin et al., Hard x-ray and Metric/Decimetric Radio Observations of the 20 February 2002 Solar Flare, *Solar Phys.*, **210**, 261-272, 2002.

Email address of N. Vilmer Nicole.Vilmer@obspm.fr

Manuscript received 19 December, 2002; revised 8 April, 2003; accepted 9 April, 2003